Yikui Liu, Student Member, IEEE, Lei Wu, Senior Member, IEEE, Yonghong Chen, Senior Member, IEEE, Jie Li, Member, IEEE, Yafei Yang, Member, IEEE

Abstract—In Independent System Operator's (ISO) energy market clearing process, sub-transmission/primary distribution systems are usually modeled as simplified fixed or flexible loads. This simplification, however, may not be proper for emerging distribution systems with an increasing penetration of distributed energy resources (DER). As a matter of fact, scheduling results from the simplified model could induce power flow violations of distribution lines, while also misrepresenting contributions of DERs on economic operations of the entire grid. To this end, this paper proposes a multi-port power exchange model and associated bidding strategies, in order to accurately and compactly formulate the contribution of highly DER-penetrated sub-transmission/distribution systems in the ISO energy market while resolving computational complexity. The proposed models can effectively capture physical and economic impacts of subtransmission/distribution systems in the ISO market clearing, while respecting their internal physical limits. Numerical studies show that, with proper settings, the proposed approach can accurately reflect impacts of DER-penetrated distribution networks on market clearing results and power flows, while presenting high computational performance.

Index Terms—Distributed energy resources, distribution system integration, unit commitment, energy market.

I. Introduction

N today's electricity energy market, Independent System 1 Operators (ISO) usually simplify sub-transmission and primary distribution systems (which are not directly monitored or explicated modelled by ISOs) as fixed loads with forecast demands or flexible loads (FL) with energy bids [1]. By simply treating internal distributed energy resources (DER) as load modifiers, this traditional approach fully neglects internal physical limits of sub-transmission and primary distribution systems. As a matter of fact, with a rapidly increasing penetration of DERs [2]-[3], power flow patterns of subtransmission and distribution systems have been transforming from unidirectional to multidirectional [4], which may even feed energy back to the transmission system. Under this circumstance, the oversimplified model may derive dispatch instructions that would potentially result in line congestion and renewable DER curtailments [5]-[6], which also fails to capture economic features of DERs in those systems.

This paper is motivated by a practical difficulty faced by ISOs that some sub-transmission/distribution systems, as well

This work was supported in part by the U.S. National Science Foundation grants CNS-1915756 and ECCS-1952683. Y. Liu, L. Wu, and Y. Yang are with ECE Department, Stevens Institute of Technology, Hoboken, NJ, 07030 USA. (E-mail: yliu262, lei.wu@stevens.edu). Y. Chen is with Midcontinent Independent System Operator, Inc., Carmel, IN, 46032 USA. J. Li is with ECE Department, Rowan University, Glassboro, NJ, 08028 USA.

Disclaimer: The views expressed in this paper are solely those of the authors and do not necessarily represent those of MISO.

as FLs and DERs inside them, are not explicitly modeled. Instead, these resources are modelled as fixed loads or flexible loads at their interconnection buses to the transmission system, together with pre-defined participation factors to approximate their impacts on power flows of the transmission network. However, a potential weakness is that the actual power consumptions of these resources could greatly deviate from dispatch instructions on interconnection buses from the ISOs, because of low economic efficiency and/or line flow congestions induced by these instructions. One major cause behind this deviation is the ignoration of sub-transmission/distribution networks and the oversimplified bidding models.

We focus on sub-transmission and primary distribution systems inside ISOs' control areas, but are not directly monitored or explicitly modeled by ISOs. Voltage levels of sub-transmission systems could typically be 110kV and 60kV, and that of primary distributions could be 35kV and 12kV, which means only mid-voltage level distribution systems are considered. These targeted systems could connect to the transmission network via multiple interconnection buses, such as those in urban areas with enhanced reliability. For the convenience of presentation, in the remaining of the paper, the term distribution system is used to refer to the targeted sub-transmission and primary distribution systems.

One intuitive solution for the above difficulty is to fully model distribution systems as well as DERs and FLs inside them. However, In the current practice, ISOs do not collect configuration details of individual DERs and FLs, such as installed capacities and interconnection statuses. Indeed, it would be challenging for individual owners of DERs and FLs to constantly update dynamic information, such as available generation of DERs, with ISOs directly, and bid them in the energy market. Even if real-time information of DERs and FLs is made available to ISOs, it is a non-trivial task to validating uploaded data, exhaustively model all DERs and FLs, together with detailed distribution system topology, into the ISO energy market clearing tool. Specifically, dispatch variables of all DERs and FLs have to appear in individual transmission line flow constraints. This would pose significant computational burden to ISO's energy market clearing tool.

Therefore, it is highly desired to build a compact model for the ISO energy market clearing, which can accurately simulate their physical and economic impacts to the transmission system while respecting their internal operation constraints, such as line flow limits and dispatch ranges of DERs and FLs. In this way, individual DERs can indirectly interact with the ISO energy market through the compact model, while remaining effectively managed by the DSO. That is, with awarded power from the ISO energy market, the DSO can self-schedule all assets within its territory to pursue security

and economic benefits. In addition, the proposed model shall be compatible to the current ISO energy market practice, and do not require additional data (i.e., data that are either currently unavailable or hard to be obtained) to achieve practical applicability.

ISOs' current practice on transmission-distribution coordination under the context of proliferated DERs was reviewed in [7]. Specifically, with an increasing penetration of DERs, distribution system operators (DSO) have been shifting from a passive to an active role to reliably operate the system and economically manage all interconnected assets [7].

In academia, bilevel models represent a mainstream to study the ISO-DSO coordination [8]-[9]. Under this framework, the ISO energy market is modeled in the upper level, while physical limitations and economic features of distribution systems are addressed in the lower level. The two levels are coupled via market clearing prices, with which the DSO optimizes DER operations/power consumptions and in turn impacts the ISO market clearing result. The bilevel models are usually solved via an iterative process, which, however, is not consistent with the current ISO energy market practice (in the sense that the ISO energy market clearing is already computationally expensive, and an iterative process on top of it will easily violate strict time limit and not be practically applicable). Another type of bilevel models separate the upper and lower level problems to the ISO and DSOs. In each iteration, dispatch instructions and prices are calculated and distributed by the ISO, according to which the DSOs can revise their bids and send them back to the ISO for the next iteration of market clearing [10].

Different from the current energy market clearing process, some references designed new market frameworks to address the DER integration problem [11]-[12]. Reference [11] proposed a model to schedule distribution systems via a dual-horizon rolling manner. Reference [12] proposes three market designs, including a sequential procurement timeline and the tailored mechanisms between the ISO and DSO. Although these frameworks present certain merits, they may be unlikely to replace the current ISO market practice.

Reference [13] represents the idea of approximating distribution systems in the ISO energy market with linear functions, which describe the relationship between operating costs of the distribution system and power injections to the ISO. Reference [14] depicted the operating boundary with respect to net power injections, including both active and reactive power, while considering operation constraints of distribution systems. However, the approaches proposed in [13]-[14] both assume single bus interconnection of distribution systems, which could become invalid when multiple interconnection buses present.

In this paper, the targeted systems are modeled via a compact multi-port power exchange model and the associated bidding strategies, which simultaneously simulate physical and economic operation features of distribution systems. Specifically, the multi-port power exchange model is constructed based on feasible operation region of the distribution system, describing physical characters of DERs,

FLs, and the distribution network; the bidding strategy model describes total operating cost of the distribution system while recognizing coupled electrical injections of multiple interconnection buses. Numerical studies show that the proposed models could bring computational benefits and achieve solutions of high accuracy. That is, results on awarded power and operation cost of distribution systems as well as line flows of transmission and distribution networks from the proposed approach align with those when the full distribution system is explicitly modelled in the ISO energy market model.

The contribution of this paper is twofold:

- 1) Particularly standing on the perspective of ISOs and paying special attention on the practical applicability and compatibility with the current ISO energy market model, effective models of DER penetrated sub-transmission/distribution systems are proposed, which are compatible to and can be directly integrated into the current ISO energy market operations. The proposed model resolves the obstacles that configuration details of DERs and sub-transmission/distribution networks are unrevealed to the ISO, and that no iterative interaction between DSOs and the ISO is practically implementable.
- 2) In the proposed integration method, a compact multi-port power exchange model and an associated bidding model are proposed, which can simultaneously simulate physical operation and economic features of sub-transmission/distribution systems.

The rest of the paper is organized as follows. The multi-port power exchange model of distribution systems is discussed in Section II. The bidding strategy model with piece-wise linear and logarithmic formulations is presented in Section III. Numerical case studies are conducted in Section IV, and the conclusions are drawn in Section V.

II. MULTI-PORT POWER EXCHANGE MODEL

In this paper, we consider a full network containing one transmission system and multiple interconnected distribution systems. Each distribution system can be in either radial or looped topology, and is connected to the transmission system via multiple interconnection buses through step-down transformers. We refer locations of step-down transformers as ports in this paper. An illustrative example is shown in Fig. 1.

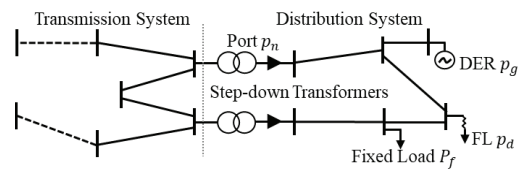


Fig. 1. An illustrative example of the system topology.

For the sake of discussion, indices of distribution systems and time intervals are not explicitly presented in the following formulations, but the proposed model can be naturally extended to multiple distribution systems and multiple time intervals. Notations \mathcal{I} , \mathcal{L} , \mathcal{G} , \mathcal{D} , and \mathcal{F} denote sets of buses, lines, DERs, FLs, and fixed loads in a distribution system, which are respectively indexed by i, l, g, d, and f; \mathcal{G}_i , \mathcal{D}_i , and \mathcal{F}_i denote sub-sets of corresponding assets connected at bus i;

 $\mathcal{N}=\{1,\ldots,N\}$ denotes the set of ports and is indexed by n; variables p_g and p_d denote dispatches of DRE g and FL d; P_f represents demand level of fixed load f; variable p_n denotes power flow injection into the distribution system through port n. Cap $\hat{\cdot}$ is used to indicate known solution of a variable.

A. The Idea of Multi-Port Power Exchange Model

We consider a situation that the ISO has network data of all interconnected distribution systems, and thus can build shift factor (SF) matrix [15] of the entire network (i.e., transmission network plus all distribution networks). The detailed SF calculation procedure can be referred to from [16]. As shown in Fig. 2, by setting one transmission bus as reference, SF matrix of the entire network includes four blocks:

- Transmission-to-Transmission (TT) Block calculates impacts of net power injections of transmission buses to power flows on transmission lines;
- Transmission-to-Distribution (TD) Block calculates impacts of net power injections of transmission buses to power flows on distribution lines;
- Distribution-to-Transmission (DT) Block calculates impacts of net power injections of distribution buses to power flows on transmission lines;
- Distribution-to-Distribution (DD) Block calculates impacts of net power injections of distribution buses to power flows on distribution lines of all distribution systems.

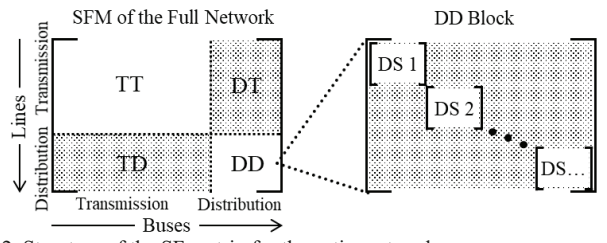


Fig. 2. Structure of the SF matrix for the entire network

To this end, in the ISO energy market clearing model, each transmission line constraint can be formulated via the corresponding row of TT and DT blocks, and each distribution line constraint can be formulated via the corresponding row of TD and DD blocks, together with power dispatch variables of all assets in transmission and distribution systems. However, in practice, the ISO may not know dynamic information of DERs, FLs, and fixed loads at individual buses of distribution systems. Moreover, including all distribution line constraints as well as dispatch variables of DERs and FLs in the ISO's energy market clearing model would introduce significant computational complexity. Thus, it is desirable to compactly model distribution systems in the ISO energy market.

The following approximations are adopted to build the proposed compact multi-port power model:

• The TD block can be reasonably approximated as zeros. This can be justified by the fact that per unit length reactance values of distribution lines and step-down transformers are comparable to that of long transmission lines. Thus, in per unit value, per unit length reactance of distribution lines are much larger than those of transmission lines, because reactance bases of different voltage levels are proportional to the square

of the voltage with the same MVA base. Since power flows are distributed according to reactance, when injecting power into a transmission bus and withdrawing from the reference bus (which is also a transmission bus), the corresponding power flows through distribution lines of a multi-port distribution system would be negligible.

- For the same reason discussed for the TD block, shift factors of a distribution line with respect to buses of other distribution systems are also negligible. Thus, all off-diagonal sub-blocks of the DD block (i.e., the shaded area shown in Fig. 2) can be approximated as zeros. The diagonal sub-blocks represent SFs of individual distribution systems.
- Since the transmission system and distribution systems exchange power through ports (i.e., all the power injections of the distribution network are eventually injected into the transmission network through the ports), the overall impacts of all asserts in a distribution system on a transmission line can be approximated as the product of p_n and the corresponding shift factors of interconnection buses in the TT block. With that, the DT block is not needed.

In summary, the TD block, the DT block, and the off-diagonal sub-blocks of the DD block, as shaded in Fig. 2, are approximated as zeros.

With the above assumptions, a transmission line constraint can be formulated via the corresponding row of the TT block, together with dispatch variables of transmission system assets and p_n of interconnection buses; similarly, a distribution line constraint is only related to the corresponding row from the DD block and dispatch variables of assets in its own distribution system. We note that the diagonal sub-blocks of the DD block are obtained from the SF matrix of the entire network, which are different from those calculated by only considering individual distribution systems.

To this end, in the ISO energy market, each distribution system can be compactly modeled via net power injection variables p_n ($n \in \mathcal{N}$) as shown in Fig. 3, together with a set of linear constraints (1) that only use p_n to describe physical operation features of distribution systems. Constraint (1) is in a general form representing a set of " \leq " inequality constraints, where $A_{h,n}$ represents the generated coefficient to p_n and B_h represents the generated constant term; \mathcal{H} denotes the set of generated constraints, indexed by h. We denote the feasible region enclosed by constraint (1) as \mathcal{P} .

Constraint (1) is constructed via the diagonal sub-blocks of the DD block by individual DSOs, and therefore called a multi-port power exchange model. The detailed procedure to derive (1) will be discussed in the next subsection. Two features of the multi-port power exchange model (1) are highlighted as follows:

- Coefficients $A_{h,n}$ and B_h in constraint (1) are generated via a variable elimination process using the original feasible operation region of the distribution system, and therefore they do not necessarily have proper physical meanings.
- Constraint (1) describes the electrical coupling between p_n ($n \in \mathcal{N}$) of multiple ports. It guarantees that if \hat{p}_n is a

feasible solution to (1), there must exist \hat{p}_g and \hat{p}_d , such that \hat{p}_n , \hat{p}_g , and \hat{p}_d together represent a physically feasible operation status of the distribution system.

$$\sum_{n \in \mathcal{N}} A_{h,n} \cdot p_n \le B_h; \qquad h \in \mathcal{H}$$
 (1)

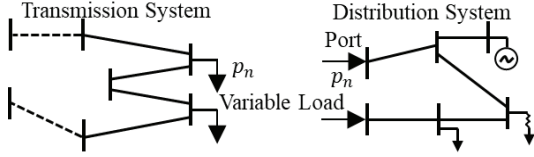


Fig. 3. Example of a multi-port power exchange model

In summary, the ISO energy market clearing with the proposed multi-port power exchange model can be solved as follows: (i) DD blocks of distribution systems are calculated by the ISO in a centralized way and released to the DSOs, with which each DSO prepares the multi-port power exchange model (1) and submits it to the ISO; (ii) the ISO solves the energy market model, which incorporates multi-port power exchange models (1) of individual distribution systems to reflect their physical operation characters, and also includes p_n and corresponding elements of the TT block in transmission line constraints to simulate impacts of distribution systems on transmission line power flows.

B. Construct the Multi-Port Power Exchange Model

With the diagonal sub-block of DD block corresponding to a distribution system released by the ISO, its feasible operation region can be formulated as in (2)-(6), with variables p_n , p_g , and p_d . Power flows on internal distribution lines are constrained by (2), while power flows on ports p_n are written as in (3) and constrained by (4), where $SF_{l,i}/SF_{n,i}$ is shift factor of bus i to line l/port n from the diagonal subblock of DD block, and F_l^{UB} and F_n^{UB} are capacity limits of distribution line l and port n. $[P_g^{LB}, P_g^{UB}]$ and $[P_d^{LB}, P_d^{UB}]$ in (5)-(6) describe dispatch ranges of DER g and FL g. It is noteworthy that power balance of the distribution system is implicated by constraint (3).

$$\begin{split} -F_{l}^{UB} &\leq \sum_{i \in \mathcal{I}} SF_{l,i} \cdot \left(\sum_{g \in \mathcal{G}_{i}} p_{g} - \sum_{d \in \mathcal{D}_{i}} p_{d} - \sum_{f \in \mathcal{F}_{i}} P_{f}\right) \\ &\leq F_{l}^{UB} \; ; \qquad l \in \mathcal{L} \qquad (2) \\ p_{n} &= \sum_{i \in \mathcal{I}} SF_{n,i} \cdot \left(\sum_{g \in \mathcal{G}_{i}} p_{g} - \sum_{d \in \mathcal{D}_{i}} p_{d} - \sum_{f \in \mathcal{F}_{i}} P_{f}\right); \\ &\qquad \qquad n \in \mathcal{N} \qquad (3) \\ -F_{n}^{UB} &\leq p_{n} \leq F_{n}^{UB}; \qquad n \in \mathcal{N} \qquad (4) \\ P_{g}^{LB} &\leq p_{g} \leq P_{g}^{UB}; \qquad g \in \mathcal{G} \qquad (5) \\ P_{d}^{LB} &\leq p_{d} \leq P_{d}^{UB}; \qquad d \in \mathcal{D} \qquad (6) \end{split}$$

Constraints (2)-(6) are used to construct the multi-port power exchange model (1) via two steps: (i) equality constraints (3) are reformatted in a row echelon form by Gaussian elimination, to substitute part of p_g and p_d in other constraints; (ii) Fourier-Motzkin elimination further discards remaining p_g and p_d in other constraints iteratively. The detained steps of Gaussian elimination and Fourier-Motzkin elimination can be referred to from references [17] and [18].

A well-recognized shortcoming of *Fourier-Motzkin elimination* is its exponential complexity in theory. We adopt three strategies to filter out redundant constraints generated in each iteration, thereby mitigating the growth of inequality

constraints and accelerating the algorithm:

- (i) *Imbert's Acceleration Theorems*: This method is a widely applied strategy with low computational efforts. It keeps track on ancestor constraints, and a new constraint is considered redundant if certain conditions are satisfied by its ancestors. Details of this method can be referred to from reference [18].
- (ii) Boundary Filtering: Upper and lower bounds of variables in (4)-(6) can be used to perform another layer of redundant constraint filtering with low computational efforts. That is, for a constraint in the standard "≤" form, its maximum possible value can be calculated by substituting the variable with a positive/negative coefficient via its upper/lower bound. If strictly less than still holds with the maximum possible value, this constraint is redundant and can be dropped.
- (iii) Linear Programming (LP) Filtering: It applies the same idea as Boundary Filtering in identifying redundant constraints, while using LP based optimization approach to identify a tighter maximum possible value. Specifically, the maximum possible value of a constraint can be calculated by maximizing this constraint term as the objective, subject to all remaining constraints [19]. This method has a stronger filtering ability with higher computational burden.

The flowchart of the algorithm is shown in Fig. 4. After *Gaussian elimination*, the remaining variables to be further eliminated are removed iteratively via *Fourier-Motzkin elimination*. The number of iterations is equal to the number of variables to be eliminated. In each iteration, one variable is eliminated, and some constraints will be generated concomitantly; then these three strategies are implemented sequentially to filter out redundant constraints. In the sequential way, strategies with higher computational complexity will be merely applied on only a few stubborn constraints.

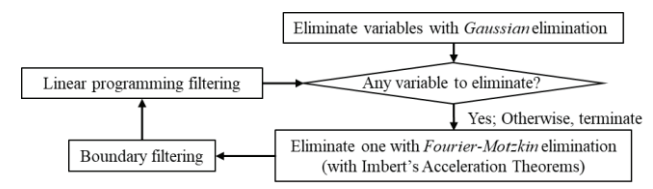


Fig. 4. Flowchart of the variable elimination process

C. Discussions on Modeling Errors and Approximation Errors

Line flow calculation errors stem from two sources, one is the modeling error when using SF to simulate distribution networks, and the other one is the approximations by setting TD block, DT block, and off-diagonal sub-blocks of DD block to zeros.

In order to make the integration model compatible with the existing energy market model which adopts a SF based DC power flow model, the same SF based DC power flow model is also used to simulate the distribution network. This, however, could result in higher calculation errors than the transmission network. Specifically, for networks with higher voltage levels such as 110kV and 60kV, this error could be small, but will become more noticeable for 35kV and 12kV networks. Of course, the magnitude of such errors eventually

depends on parameters of lines in the network.

The proposed multi-port power exchange model may induce errors to line flows for both the transmission and distribution networks, due to the approximations adopted in Section II.A, which would be our focus for further discussion. Firstly, approximating the TD block as zero (i.e., ignoring impacts of transmission bus injections on distribution lines) could introduce errors on power flows of distribution systems. Two factors impact the magnitude of such line flow errors: (i) significance of shift factors in the original TD block, and (ii) magnitudes of power injections at transmission buses. The fact that elements in the TD block are relatively small is considered as a prerequisite to apply the proposed multi-port power exchange model.

Secondly, equating a distribution system as variable loads with corresponding shift factors in the TT block would induce power flow errors of transmission lines. The reason is that, in order to achieve exact power flows of transmission lines under this equivalence, one shall use shift factors of interconnection buses corresponding to a network excluding this distribution system. Those values are slightly different from the elements in the TT block which are calculated corresponding to the full network and thus consider flow diversion of all distribution systems. Indeed, such differences could become relatively larger for transmission lines closer to interconnection buses.

Lastly, setting off-diagonal sub-blocks of the DD block as zeros ignores the interaction between distribution systems, which, although very tiny, could still result in certain level of line flow errors on distribution lines.

The approximation errors will be quantitively analyzed in numerical studies. It is also noteworthy that line flow errors can be effectively avoided in certain special occasions. One example is when all ports are connected at a single interconnection bus of the transmission network, as shown in Fig. 5. Another occasion is when N=1, namely a single port.

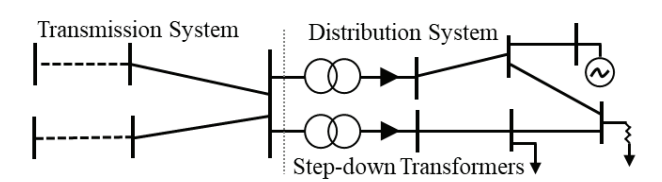


Fig. 5. An example of special occasions without line flow errors

III. MULTI-PORT BIDDING STRATEGY MODEL

The multi-port power exchange model discussed above focuses on physical operation features of distribution systems, which restricts physical feasibility of power dispatches p_n in the market clearing while not describing any economic information. As a bid in the ISO energy market always includes two-part information, the quantity and the price, a bidding model over p_n has to be supplemented to address economic features of distribution systems.

To this end, in this section, a bidding model construction approach is proposed. With price information from DERs and FLs in a distribution system, this approach can help the DSO construct a bidding model submitted to the ISO, together with

the multi-port power exchange model, for energy market clearing. For the sake of discussion, a single price for each DER/FL is considered.

The operating cost of a distribution system in the ISO energy market is jointly determined by p_n of all ports. With given \hat{p}_n ($n \in \mathcal{N}$) inside \mathcal{P} , namely satisfying (1), the total operating cost of the distribution system can be optimized via a self-dispatch problem (7)-(9), where C_g/C_d is the price of DER $g/\text{FL}\ d$. Therefore, the operating cost is a function of p_n over the entire \mathcal{P} and can be denoted as $C(\hat{p}_n)$. Any \hat{p}_n outside \mathcal{P} will not be awarded, as restricted by the multi-port power exchange model. As $C(p_n)$ is related to the optimal solution to (7)-(9) over the entire \mathcal{P} , its analytical form may not be obtained easily.

To this end, we plan to approximate the cost function via a piecewise linear function, in which the operating cost is linearly associated with p_n ($n \in \mathcal{N}$), thereby integrable to the ISO energy market model. Two alternative formulations, i.e., piecewise formulation and logarithmic formulation [20], are introduced to build the piecewise linear function. In the following discussions, we start with the case of N = 1, then extend to cases of N = 2 and $N \geq 3$.

$$\min C(\hat{p}_n) = \sum_{g \in \mathcal{G}} C_g \cdot p_g - \sum_{d \in \mathcal{D}} C_d \cdot p_d \tag{7}$$

Constraints (2) and (5)-(6);
$$(8)$$

$$\hat{p}_{n} = \sum_{i \in \mathcal{G}} SF_{n,i} \cdot \left(\sum_{g \in \mathcal{G}_{i}} p_{g} - \sum_{d \in \mathcal{D}_{i}} p_{d} - \sum_{f \in \mathcal{F}_{i}} P_{f} \right);$$

$$n \in \mathcal{N}$$
(9)

A. 1-D Bidding Model

For the case of N=1, the approximated piecewise function is univariate on p_1 , and is not necessarily monotonically increasing. We set the number of equidistant segments as 2^M , for an integer parameter M. The set of segments is collected in $S = \{1, ..., 2^M\}$, and indexed by s. The set of endpoints is denoted as $K = \{1, ..., 2^{M+1}\}$, and indexed by k and k'. In the one-dimensional space, these segments are 2-simplexes, thereby each endpoint corresponds to a vertex and is associated with variable λ_k . Finally, we use set J^2 to collect all 2-simplexes and index them by J. The neighbor simplex of a vertex refers to a simplex that contains this vertex. Neighbor 2-simplexes of a vertex J^2 are collected in set J^2 .

• Piecewise Formulation can be represented as in (10)-(15). Operating cost of the distribution system is calculated in (10), where C_k^V is operating cost corresponding to vertex k. Importantly, this term shall be included in the objective of the ISO energy market to represent economic feature of the distribution system. Constraint (11) defines simplexes. Constraint (12) calculates p_1 , i.e., power flow through the port, where $P_{1,k}^V$ is the value of p_1 at vertex k. Constraint (13) forces one and only one simplex to be active, where binary variable μ_j indicates status of 2-simplex j (i.e., 1: active, 0: inactive). Constraint (14) forces λ_k within [0,1], and to be non-zero only if one of its neighbor simplexes is active. Constraint (15) defines binary variables.

$$\sum_{k \in \mathcal{K}} C_k^V \cdot \lambda_k; \tag{10}$$

$$\sum_{k \in \mathcal{K}} \lambda_k = 1; \tag{11}$$

$$p_1 = \sum_{k \in \mathcal{K}} P_{1,k}^V \cdot \lambda_k; \tag{12}$$

$$\sum_{j \in \mathcal{J}^2} \mu_j = 1; \tag{13}$$

$$0 \le \lambda_k \le \sum_{j \in \mathcal{J}_k^2} \mu_j; \qquad k \in \mathcal{K}$$
 (14)

$$\mu_j \in \{0,1\}; \qquad \qquad j \in \mathcal{J}^2 \qquad (15)$$

• Logarithmic Formulation maps a full set of M-bit Gray code (2^M codes) to the 2^M segments in sequence. We represent the code corresponding to segment s as R_s . Set \mathcal{V} , defined as $\{1...M\}$, is mapped with bits of the M-bit Gray code. Operator $sup(\cdot)$ returns non-zero bits of a Gray code. $v \in sup(\cdot)$ is true if bit v is included in the returned non-zero bits; otherwise, it is false. Furthermore, S_k means the set of segments that contain endpoint k. It is clear that cardinality of S_k is either 1 or 2. The logarithmic formulation is built by replacing (12)-(15) with (16)-(19), where indicator $u_{1,v}$ identifies the active 2-simplex jointly.

$$\sum_{k \in \{k' \in \mathcal{K} | \forall s \in \mathcal{S}_{k'}, \nu \in sup(R_s)\}} \lambda_k \leq u_{1,\nu}; \qquad \nu \in \mathcal{V} \qquad (16)$$

$$\sum_{k \in \{k' \in \mathcal{K} | \forall s \in \mathcal{S}_{k'}, \nu \notin sup(R_s)\}} \lambda_k \leq 1 - u_{1,\nu}; \qquad \nu \in \mathcal{V} \qquad (17)$$

$$0 \leq \lambda_k \leq 1; \qquad k \in \mathcal{K} \qquad (18)$$

$$u_{1,\nu} \in \{0,1\}; \qquad \nu \in \mathcal{V} \qquad (19)$$

Comparing with the piecewise formulation which introduces 2^M binary variables and 2^M+1 continuous variables, logarithmic formulation only introduces M (i.e., $\log_2(2^M)$) binary variables and has the same number of continuous variables. Consequently, a higher computation performance is expected.

B. 2-D Bidding Model

When N=2, \mathcal{P} becomes a polygon in the two-dimensional rectangular coordinates as shown in Fig. 6. We approximate the bivariate cost function within a triangulated square domain in the Union Jack structure, as the grid of dashed lines shown in Fig. 6. That is, \mathcal{P} is divided by 3-simplexes arranged in a specific structure, and cost of any point in a 3-simplex can be linearly approximated via values of its three vertices.

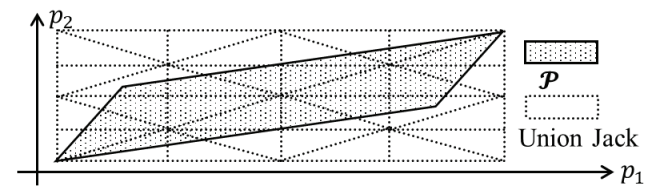


Fig. 6. Polygon of $\boldsymbol{\mathcal{P}}$ and the Union Jack structure

The numbers of equidistant segments on the two dimensions are both set as 2^M . Therefore, definitions of $\mathcal S$ and $\mathcal K$ can be applied on each of the two dimensions. Each vertex of the grid is uniquely tagged by a pair of coordinates $(k,k') \in \mathcal K$, and associated with variable $\lambda_{k,k'}$. Furthermore, the definition of $\mathcal J^3$ remains the same but collects 3-simplexes, while $\mathcal J^2_k$ is expanded to $\mathcal J^3_{k,k'}$ to collect neighbor 3-simplexes of vertex (k,k').

• Piecewise Formulation is presented as in (20)-(25), similar to constraints (10)-(15) of the 1-D bidding model. $C_{k,k'}^V$ and $P_{n,k,k'}^V$ are the operating cost and the value to p_n $(n \in \{1,2\})$ at vertex (k,k'); binary variable μ_i works similarly

as (13)-(14) in the 1-D bidding model, but indicates 3-simplexes in the 2-D bidding model.

$$\sum_{k,k'\in\mathcal{K}} C_{k,k'}^V \cdot \lambda_{k,k'}; \tag{20}$$

$$\sum_{k,k'\in\mathcal{K}} \lambda_{k,k'} = 1; \tag{21}$$

$$p_n = \sum_{k,k' \in \mathcal{K}} P_{n,k,k'}^V \cdot \lambda_{k,k'}; \qquad n \in \{1,2\}$$
 (22)

$$\sum_{j \in \mathcal{J}^3} \mu_j = 1; \tag{23}$$

$$0 \le \lambda_{k,k'} \le \sum_{j \in \mathcal{J}_{k,k'}^3} \mu_j; \qquad k, k' \in \mathcal{K}$$
 (24)

$$\mu_j \in \{0,1\}; \qquad \qquad j \in \mathcal{J}^3 \tag{25}$$

• Logarithmic Formulation is built by replacing (22)-(25) with (26)-(34). Besides applying a full set of M-bit Gray code and defining \mathcal{V} and \mathcal{S}_k on each dimension, set \mathcal{K} is divided into two sub-sets of \mathcal{K}^{EVE} and \mathcal{K}^{ODD} , respectively containing even and odd values in \mathcal{K} . In constraints (26)-(31), the indicators are expanded to binary variables $u_{1,v}, u_{2,v}$, and z. Their combination ultimately identifies the active 3-simplex, forcing all $\lambda_{k,k}$, as zero except those three in the active 3-simplex. It is emphasized that the logarithmic formulation is specific for grids in the Union Jack structure. In the grid, $u_{1,v}$ and $u_{2,v}$ reduce choices of 3-simplexes in a way of dichotomy on two dimensions, and finally locate to two 3-simplexes in a small square. Finally, variable z decides which 3-simplex will be picked up.

$$\sum_{k \in \mathcal{K}} \sum_{k' \in \{k'' \in \mathcal{K} | \forall s \in \mathcal{S}_{k''}, v \in sup(R_s)\}} \lambda_{k,k'} \le u_{1,v}; \quad v \in \mathcal{V} \quad (26)$$

$$\sum_{k \in \mathcal{K}} \sum_{k \in \{k'' \in \mathcal{K} | \forall s \in \mathcal{S}_{k''}, v \in sup(R_s)\}} \lambda_{k,k'} \leq u_{2,v}; \quad v \in \mathcal{V}$$

$$\sum_{k \in \mathcal{K}} \sum_{k' \in \{k'' \in \mathcal{K} | \forall s \in \mathcal{S}_{k''}, v \notin sup(R_s)\}} \lambda_{k,k'} \leq 1 - u_{1,v};$$

$$(27)$$

$$v \in \mathcal{V} \quad (28)$$

$$\textstyle \sum_{k' \in \mathcal{K}} \sum_{k \in \{k'' \in \mathcal{K} | \forall s \in \mathcal{S}_{k''}, v \notin sup(R_s)\}} \lambda_{k,k'} \leq 1 - u_{2,v};$$

$$v \in \mathcal{V}$$
 (29)

$$\sum_{k \in \mathcal{K}^{EVE}, k' \in \mathcal{K}^{ODD}} \lambda_{k,k'} \le Z; \tag{30}$$

$$\sum_{k \in \mathcal{K}^{ODD}, k' \in \mathcal{K}^{EVE}} \lambda_{k,k'} \le 1 - z; \tag{31}$$

$$0 \le \lambda_{k,k'} \le 1; \qquad k, k' \in \mathcal{K} \quad (32)$$

$$u_{1,v}, u_{2,v} \in \{0,1\};$$
 $v \in \mathcal{V}$ (33)
 $z \in \{0,1\};$ (34)

It can be seen that the piecewise formulation assigns one binary variable to each 3-simplex to indicate its active/inactive status, while the logarithmic formulation uses two set of binary variables to jointly decide a 3-simplex's active/inactive status with binary encoding. In this case, piecewise formulation introduces $2^{2\times M+1}$ binary variables, while logarithmic formulation only introduces $2^{\times M+1}$ binary variables, i.e., $\log_2(2^{2\times M+1})$. They have the same number of $(2^M+1)^2$ continuous variables.

Table I summarizes constraints of the two formulations under 1-D and 2-D bidding situations.

TABLE I. SUMMARY OF PIECEWISE AND LOGARITHMIC FORMULATIONS

Formulation	1-D bidding	2-D bidding
Piecewise Formulation	(10)-(15)	(20)-(25)
Logarithmic Formulation	(16)-(19)	(26)-(34)

Computational performance of the 2-D bidding model is further discussed as follows:

• Invalid Vertices: Firstly, the cost function is approximated within a triangulated square domain that covers the polygon of \mathcal{P} , as shown in Fig. 6. Some vertices in the grid are outside of

the polygon of \mathcal{P} , which indicates their corresponding \hat{p}_n are not allowed by the multi-port power exchange model and infeasible to (7)-(9), and thereby no valid $C_{k,k'}^V$ is available. To address it, we set all $\lambda_{k,k'}$ corresponding to vertices outside of \mathcal{P} as zero, i.e. $\lambda_{k,k'}=0$. In this way, a 3-simplex crossing the boundary of the region is essentially degenerated to an edge if two vertices are valid (see the shadow triangle on the right in Fig. 7), or a point if only one vertex is valid (see the shadow triangle on the left in Fig. 7). Finally, a new boundary shown as the dashed lines in Fig. 7 can be formed.

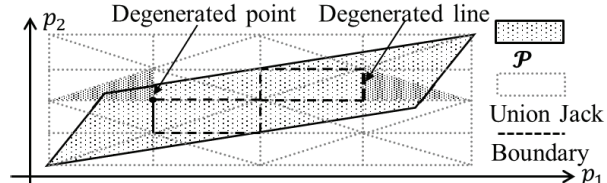


Fig. 7. An illustration of a new boundary after excluding invalid vertices

High Ratio of Invalid Vertices: Another issue is that the ratio of invalid vertices over all vertices in the triangulated domain could be high, as the example in Fig. 6, while these vertices outside of \mathcal{P} do not contribute to improving the linearization accuracy. This appears because the vertical square domain poorly fits the polygon of $\boldsymbol{\mathcal{P}}$ that is oblique to the coordinate axis as in Fig. 6. If the square domain can be rotated by a certain angle and scaled adaptively, more vertices will be located inside \mathcal{P} and become valid. This is shown in Fig. 8. Here, we propose to solve the problem (35)-(41), in order to find a square domain that overlaps with the polygon as much as possible, as shown in Fig. 8. The objective (35) is to minimize the area of the encircled rectangle. In this problem, two base lines are represented in the form of y = $\alpha_1 \cdot x + \beta_1$ and $y = \alpha_2 \cdot x + \beta_2$, with $\alpha_1, \alpha_2, \beta_1$, and β_2 as variable coefficients. The two lines are perpendicular as constrained by (36). Two other lines are used by shifting the two base lines in parallel along the coordinates. The distances shifted are represented by δ_1 and δ_2 . Thus, these four lines encircle a rectangle. Constraint (37) specifies slope ranges of lines, and sets non-negative differences of intercepts to exclude solution ambiguity. Constraints (38)-(41) ensure every vertex of $\boldsymbol{\mathcal{P}}$ is inside the rectangle. Vertices of $\boldsymbol{\mathcal{P}}$, represented by $F_{1,w}^V$ and $F_{2,w}^V$, are collected in set $\boldsymbol{\mathcal{W}}$ and indexed by w. It is noteworthy that vertexes of \mathcal{P} can be obtained from (1). To this end, the grid in Union Jack structure can be filled in the obtained rectangle domain. Fig. 8 clearly shows that, in comparison with Fig. 6, with the fitted rectangle domain, more vertices of the grid (i.e., 11 versus 9) are located inside the polygon described by \mathcal{P} . Problem (35)-(41) is a small-scale nonlinear programming problem which can be effectively solved by commercial nonlinear solvers.

$$min \, \delta_1 \cdot \delta_2$$
 (35)

$$\alpha_1 \cdot \alpha_2 = -1; \tag{36}$$

$$\alpha_1 \ge 0; \, \alpha_2 \le 0; \, \delta_1 \ge 0; \, \delta_2 \ge 0; \tag{37}$$

$$F_{2,w}^V - \alpha_1 \cdot F_{1,w}^V - \beta_1 \ge 0; \qquad w \in \mathcal{W}$$
 (38)

$$\alpha_{1} \quad \alpha_{2} = 1,$$

$$\alpha_{1} \geq 0; \ \alpha_{2} \leq 0; \ \delta_{1} \geq 0; \ \delta_{2} \geq 0;$$

$$F_{2,w}^{V} - \alpha_{1} \cdot F_{1,w}^{V} - \beta_{1} \geq 0;$$

$$W \in \mathcal{W}$$

$$(39)$$

$$F_{2,w}^{V} - \alpha_{2} \cdot F_{1,w}^{V} - (\beta_{1} + \delta_{1}) \leq 0;$$

$$W \in \mathcal{W}$$

$$(39)$$

$$F_{2,w}^V - \alpha_2 \cdot F_{1,w}^V - \beta_2 \ge 0; \qquad \qquad w \in \mathcal{W} \tag{40}$$

$$F_{2,w}^{V} - \alpha_{2} \cdot \left(F_{1,w}^{V} - \delta_{2}\right) - \beta_{2} \leq 0; \qquad w \in \mathcal{W}$$

$$y = \alpha_{1} \cdot x + (\beta_{1} + \delta_{1}) \qquad y = \alpha_{2} \cdot (x + \delta_{2}) + \beta_{2}$$

$$y = \alpha_{2} \cdot x + \beta_{2} \qquad y = \alpha_{1} \cdot x + \beta_{1} \qquad \text{Union Jack}$$

$$y = \alpha_{1} \cdot x + \beta_{1} \qquad \text{Boundary}$$

$$v = \alpha_{1} \cdot x + \beta_{1} \qquad v = \alpha_{1} \cdot x + \beta_{1} \qquad v = \alpha_{1} \cdot x + \beta_{1}$$

Fig. 8. An illustration of the fitted square domain

C. Discussion on Cases of $N \ge 3$

Although most practical distribution systems can be fit in N=1 and N=2 cases, we briefly discuss cases of $N \ge 3$. For these cases, \mathcal{P} constructed from the feasible operation region of the distribution system can be represented in a higher dimensional space, which requires simplexes of higher order. For example, when N=3, $\boldsymbol{\mathcal{P}}$ represents a three-dimensional space, described via 4-simplexes. For a high-dimensional space, heterogeneous structures may be used to divide it into non-overlapping simplexes. The piecewise formulation is usually applicable to various division structures, with one binary indicating active/inactive status of each simplex [21]; while the logarithmic formulation requires a special structure, such as the Union Jack structure for a 2-dimensional domain.

IV. CASE STUDIES

A modified 1888-bus transmission system from the MATPOWER library is used to evaluate the proposed approach in terms of computational performance, economic efficiency, and solution quality (i.e., line flow errors). Modifications on the 1888-bus systems include creating 24hour load profiles, supplementing generator parameters, and revising line capacities.

In total, 10 distribution systems are interconnected to the 1888-bus system, each of which is a modified 33-bus distribution system with two ports to the transmission system. They are identical except the interconnection buses. Each distribution system contains 8 DERs and 6 FLs. Prices of DERs are set to be lower than those of thermal units in the transmission system. In each distribution system, 32 internal lines and 2 ports form a looped topology, and all lines are monitored via constraints (2)-(3). Line flow capacities are set as 5MW, which are originally sufficient to supply all loads. However, a high penetration of DERs could potentially trigger congestions. The detailed case data can be found in [22].

The ISO day-ahead energy market solves a 24-hour UC model, which is formulated as a mixed-integer linear programming (MILP) problem with the objective of minimizing the total system operating cost. The UC model contains prevailing constraints, such as generation dispatch ranges, minimum ON/OFF time, and ramping constraints at the unit level, as well as power balance and line flow constraints at the system level [23]. Four models with different methods to simulate distribution systems are studied:

Full Model (FULL Model): The full UC model by exhaustively formulating distribution systems and their internal assets. This model is regarded as the benchmark, in which line flows of the transmission system and distribution systems are calculated through the SF matrix of the full network, while DERs and FLs in distribution systems are modeled similarly as transmission system assets.

- Current Model (CUR Model): Power of distribution systems is distributed on their interconnection buses with pre-defined participation factors, and distribution system network constraints are not considered. In this case, participation factors are determined based on the result from FULL Model.
- Piecewise Formulation Model (PW Model): The proposed multi-port power exchange model (1) and the associated bidding strategies in the piecewise formulation (10)-(15)/(20)-(25).
- Logarithmic Formulation Model (LOG Model): The proposed multi-port power exchange model (1) and the associated bidding strategies in the logarithmic formulation (16)-(19)/(26)-34).

In all models, the UC formulation remains a MILP problem. All models are implemented via Yalmip [24] in MATLAB and solved by Gurobi 9.0.0 to zero MIP gap (i.e., global optimal solutions are pursued for fair comparison). Nonlinear problems (35)-(41) are solved by IPOPT [25]. All simulations are executed on a PC with i7-3.6GHz CPU and 16GB RAM.

Comparison of the Three Models

Computational Performance

Although all distribution systems have the same network configuration, because of their different interconnection locations, values of diagonal sub-blocks in the DD block and thus their \mathcal{P} regions are different. An example of the feasible region is shown in Fig. 9. It has a coniferous shape enclosed by 18 lines. That is, \mathcal{H} in (1) contains 18 constraints. The 18 circles marked in Fig. 9 are intersections of the 18 lines. The dashed rectangle that well fits $\boldsymbol{\mathcal{P}}$ is obtained from problem (35)-(41). It clearly shows that the rectangle covers the entire \mathcal{P} and only contains very limited invalid areas.

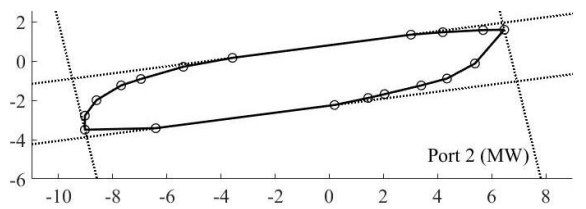


Fig. 9. An example of $\boldsymbol{\mathcal{P}}$ and its fitted rectangle domain.

A triangulation grid in Union Jack structure is then filled into the rectangle. The number of segments, 2^{M} , is of importance to define the fineness of the grid. A large r M could improve approximation accuracy of the cost function, at the cost of higher computational burden. We test different values of M from 3 to 5, corresponding to 8, 16, and 32 segments, in PW Model and LOG Model to evaluate the impacts of M on computational performance and economic efficiency.

Table II compares computational performance of the three

models. It shows that with different settings on M, objectives of PW Model and LOG Model are always identical, verifying that the two formulations are equivalent. However, as M increases, LOG Model significantly outperforms PW Model in terms of computational efficiency. In addition, in both models, a larger M requires higher computational efforts, while it derives solutions of higher quality in terms of smaller objective deviation referring to FULL Model.

Although CUR Model has slightly shorter computational time and smaller objective value, power dispatch instructions of DERs from this simplified model are infeasible to the distribution systems, i.e., capacity limits of distribution lines 20-21 and 21-22 are violated. The smaller objective value is due to the allowance of violations. However, LOG Model can avoid this issue. In addition, it can be seen that even comparing with CUR model, the increased computational time of LOG model is very limited.

Moreover, compared with FULL Model, LOG Model shows computational advantages with M of 3 and 4, but is more computational demanding when M=5. It can be concluded that the computational benefits by avoiding exhaustively modeling networks and individual assets of distribution systems may disappear when overly detailing the 2-D bidding model. Thus, a tradeoff on the value of M is inevitable. As illustrated, M=4is appropriate in this system with higher computational performance and acceptable accuracy in representing economic features. Thus, in the following studies, we focus on LOG Model with M=4 and compare it with the setting of M=3.

TABLE II. COMPUTATIONAL PERFORMANCE OF THE THREE MODELS

Model		Computational	Objective (\$)	Objective deviation against
		time (s)	σομετίτε (φ)	FULL Model (\$)
PW Model	8 (M=3)	42.67	32,522,273.38	+1,219.97
	16 (M=4)	63.36	32,521,373.53	+320.12
	32 (M=5)	95.34	32,520,757.45	-295.96
LOG Model	8 (M=3)	35.04	32,522,273.38	+1,219.97
	16 (M=4)	36.84	32,521,373.53	+320.12
	32 (M=5)	56.78	32,520,757.45	-295.96
FULI	L Model	48.03	32,521,053.41	-
CUR	Model	32.77	32,509,931.69	-

Economic Efficiency

Two metrics are used to evaluate closeness of distribution system solutions of LOG Model to FULL Model. One is average power deviation (WD) on ports of a distribution system defined as in (42), and the other is average operating cost deviation (CD) of a distribution system defined as in (43). Operator $|\cdot|$ returns the absolute value; T = 24 is the number of time intervals. In (42), $\hat{p}_{n,t}^{LOG}$ and $\hat{p}_{n,t}^{FULL}$ denote the awarded power through port n at time t from LOG Model and FULL*Model*, respectively. $\hat{p}_{n,t}^{FULL}$ can be calculated via dispatches to all assets and SF matrix of the full network. In (43), \hat{c}_t^{LOG} and \hat{c}_t^{FULL} indicate operating cost of a distribution system at time t from LOG Model and FULL Model. \hat{c}_t^{LOG} is calculated through (20), and \hat{c}_t^{FULL} equals to $\sum_{g \in \mathcal{G}} C_g \cdot \hat{p}_g - \sum_{d \in \mathcal{D}} C_d \cdot \hat{p}_d$.

$$WD_{n} = \sum_{t=1}^{T} |\hat{p}_{n,t}^{LOG} - \hat{p}_{n,t}^{FULL}|/T;$$

$$CD = \sum_{t=1}^{T} |\hat{c}_{t}^{LOG} - \hat{c}_{t}^{FULL}|/T;$$
(42)

$$CD = \sum_{t=1}^{T} |\hat{c}_t^{LOG} - \hat{c}_t^{FULL}|/T; \tag{43}$$

Clearly, a smaller value of WD/CD indicates

dispatches/operating costs from the two models are closer, verifying better economic efficiency of the proposed multiport model, that is, better ability in capturing economic features of distribution systems.

WD values of the 10 interconnected distribution systems under settings of M=3 and M=4 are shown in Fig. 10. As expected, the case of M=4 shows better economic efficiency than the case of M=3 on both ports for all distribution systems, which also explains a reduction of \$899.85 in the objective deviation as shown in Table II. The small power deviation values with M=4 verify effectiveness of the 2-D bidding model in capturing economic efficiency of distribution networks. Taken distribution network #1 at time t=1 as an example, its average total power injection through two ports over 24 hours, i.e. $\sum_{t=1}^{T} \sum_{n=1}^{2} |\hat{p}_{n,t}^{FULL}|/T$, is 10.77MW, while summation of WD_1 and WD_2 is only 0.59MW (5.48%). Moreover, average power deviations shown in Fig. 10 seem gathered on one port instead of evenly distributed on both ports. This is because of unbalanced power dispatches on the two ports, caused by electrical coupling between p_n . For instance, average power injections into distribution network #1 through the two ports are -7.61MW and -3.16MW.

Values of CD for all distribution networks under settings of M=3 and M=4 are within [\$50.76, \$55.11] and [\$13.77, \$20.55], which further verify that the case of M=4 leads to better economic performance. It is worthwhile to emphasize that operating cost deviation is positively related to the power deviation on awarded p_n .

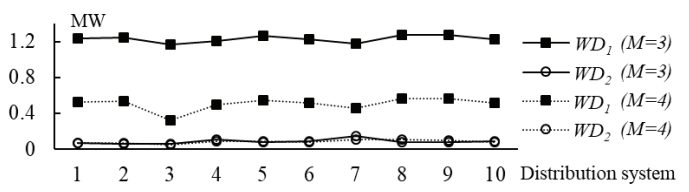


Fig. 10. Comparison of WD values for the 10 distribution systems.

B. Line Flow Error Analysis

Approximations adopted in the proposed approach would induce line flow errors. After the ISO energy market is cleared using LOG Model, power flows and generation dispatches of the transmission system, as well as awarded power on ports of the distribution systems become known. With awarded power on ports, the DSOs can self-dispatch DERs and FLs by optimizing the problem (7)-(9). Accordingly, power flows on distribution lines and dispatches of assets (DERs and FLs) inside the distribution systems can be obtained. To this end, power flows of all transmission and distribution lines are obtained, which, however, are approximated values with potential errors, because of the approximated network model.

Indeed, with dispatches of all transmission assets derived from *LOG Model* and dispatches of all distribution assets from the self-dispatch problem, actual line flows can be exactly calculated using the original SF matrix of the full network. We define the absolute differences between the approximated and the actual line flow values as line flow errors. The flowchart of the line flow comparison process is shown in Fig. 11.

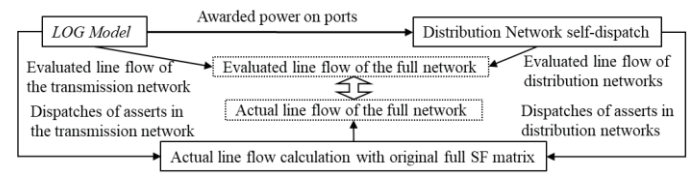


Fig. 11. Flowchart of the line flow comparison process

Fig. 12 shows the maximum line flow errors among 24 hours of individual transmission/distribution lines from Log Model with M=4. Assets #1-#2531 are lines/transformers of the transmission network, and #2532-#2571 are lines/ports of the 10 distribution systems. It shows that line flow errors in the transmission system, which are less than 0.11MW, are negligible and mainly exist on lines electrically closer to distribution systems. In comparison, larger line flow errors in distribution systems are observed. This is because line flow errors induced by ignoring the TD block are relatively larger than that induced by equating distribution networks as variable loads to the transmission system via the TT block. Levels of line flow errors among different distribution systems also vary, mainly because of their different interconnection locations in the transmission system. For instance, line flow errors of distribution system #5 (i.e., lines #2668-#2699) are more significant than others. In this case, the largest line flow error of 0.1663MW occurs on line #2698 at t=15. In fact, compared with other distribution systems, shift factors of distribution system #5 in the TD block, which is approximated as zeros and plays a major role in inducing errors, is not notable large. However, at bus #1799, the corresponding shift factor of line #2673 in the TD block is much higher than other distribution lines, and generators connected at this bus are dispatched at 605MW. These facts all together cause a line flow error of 0.0563MW, over 33% of the total flow error of this line. This explains the two main factors causing distribution line flow errors, as discussed in Section II.C.

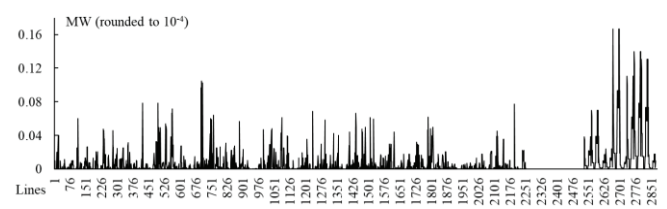


Fig. 12. Maximum line flow errors over 24 hours for each line in the full grid.

It is also noteworthy that the approximations adopted in the proposed approach could cause under or overestimations of distribution line flows. Specifically, evaluated power flows through approximations could underestimate actual flows with respect to dispatches of all transmission and distribution assets, which might have already violated their limits at certain time intervals. For example, evaluated power flow on line #2688 in distribution system #5 at t=15 is binding at its capacity limit of 5.00MW, while the actual power flow is 5.02MW. An example of overestimation also occurs at t=15, on line #2756 in distribution network #7. The evaluated and actual power flows are respectively 5.00MW and 4.98MW. However, considering these values are rather small, small headroom and floor rooms could be applied to avoid violations

in practice, while not significantly compromising operational economics.

V. CONCLUSION

This paper proposes a multi-port power exchange model and associated bidding strategies to integrate distribution systems with high penetrated DERs into the ISO energy market. The proposed models leverage physical characters of distribution networks and operating costs of DERs to compactly model distribution systems. In terms computational efficiency and solution accuracy, it is concluded that with a proper setting on M: (i) computational benefits in ISO market clearing can be achieved, and (ii) accurate solutions on awarded power and operating cost of distribution systems can be obtained. On the other hand, the proposed model is associated with line flow errors in the transmission and distribution networks. However, as line flow errors are rather small, small headroom and floor rooms can be adopted to mitigate the risks of violations for underestimated cases, while not significantly compromising operational economics for overestimated situations.

REFERENCES

- M. Shahidehpour, H. Yamin, and Z. Li, Market operations in electric power systems. New York: Wiley, 2002.
- [2] H. Wu and M. Shahidehpour, "Stochastic SCUC solution with variable wind energy using constrained ordinal optimization," *IEEE Trans. Sustain. Energy*, vol. 5, no. 2, pp. 379-388, Apr. 2014.
- [3] DoE, "Quadrennial energy review transforming the nation's electricity system: the second installment of the QER," Jan. 2017. [Online] Available: https://www.energy.gov/policy/initiatives/quadrennialenergy-review-qer/quadrennial-energy-review-second-installment.
- [4] Z. Li, M. Shahidehpour, A. Alabdulwahab, and Y. Al-Turki, "Valuation of distributed energy resources in active distribution networks," *The Electricity Journal*, vol. 32, no. 4, pp. 27-36, May 2019.
- [5] S. Y. Hadusha and L. Meeus, "DSO-TSO cooperation issues and solutions for distribution grid congestion management," *Energy Policy*, vol. 120, pp. 610-621, Sept. 2018.
- [6] R. Verzijlbergh, L. Vries, and Z. Lukszo, "Renewable energy sources and responsive demand. do we need congestion management in the distribution grid?" *IEEE Trans. Power Syst.*, vol. 29, no. 5, pp. 2119-2128, Sept. 2014.
- [7] M. Birk, J. Chaves-Ávila, T. Gómez, and R. Tabors, "TSO/DSO coordination in a context of distributed energy resource penetration," Oct. 2017. [Online] Available: http://ceepr.mit.edu/files/papers/2017-017.pdf.
- [8] H. Wu, M. Shahidehpour, A. Alabdulwahab, and A. Abusorrah, "Dayahead scheduling with variable renewable generation," *IEEE Trans. Sustain. Energy*, vol. 6, no. 2, pp. 516-525, Apr. 2015.
- [9] M. Bragin and Y. Dvorkin, "Toward coordinated transmission and distribution operations," *IEEE Power & Energy Society General Meeting (PESGM)*, Portland, OR, USA, Aug. 2018.
- [10] A. Safdarian, M. Fotuhi-Firuzabad, M. Lehtonen, and F. Aminifar, "Optimal electricity procurement in smart grids with autonomous distributed energy resources," *IEEE Trans. Smart Grid*, vol. 6, no. 6, pp. 2795-2984, Nov. 2015.
- [11] A. Saint-Pierre and P. Mancarella, "Active distribution system management: a dual-horizon scheduling framework for DSO/TSO interface under uncertainty," *IEEE Trans. Smart Grid*, vol. 8, no. 5, pp. 2186-2197, Sept. 2017.
- [12] A. Vicente-Pastor, J. Nieto-Martin, D.W. Bunn, and A. Laur, "Evaluation of flexibility markets for retailer—DSO—TSO coordination," *IEEE Trans. Power Syst.*, vol. 34, no. 3, pp. 2003-2012, May 2019.
- [13] Z. Yuan and M.R. Hesamzadeh, "Hierarchical coordination of TSO-DSO economic dispatch considering large-scale integration of distributed energy resources," *Appl. Energy*, vol. 195, no. 2, pp. 600-

- 615, Jun. 2017.
- [14] J. Silva, J. Sumaili, R.J. Bessa, et al, "Estimating the active and reactive power flexibility area at the TSO-DSO interface," *IEEE Trans. Power* Syst., vol. 33, no. 5, pp. 4741-4750, Sept. 2018.
- [15] Y. Fu and Z. Li, "Different models and properties on LMP calculations," IEEE Power & Energy Society General Meeting (PESGM), Montreal, Canada, Jun. 2006.
- [16] Calculation of shift factors, [Online] Available: http://home.Engineering.iastate.edu/~jdm/ee553/SensitivitiesGSF.pdf.
- [17] J.G. Strang, Linear Algebra and Its Application, Brooks/Cole, India, 2005.
- [18] L. Imbert, "Fourier's elimination: Which to choose?" in Proc. PPCP, 1993.
- [19] S. Paulraj and P. Sumathi "A comparative study of redundant constraints identification methods in linear programming problems," *Mathematical Problems in Engineering*, vol. 2010, pp. 1-16, 2010.
- [20] J. Vielma and G. Nemhauser, "Modeling disjunctive constraints with a logarithmic number of binary variables and constraints," *Mathematical Programming*, vol. 128, no. 1-2, pp. 49-72, Jan. 2017.
- [21] R. Misener and C. Floudas, "Piecewise-linear approximations of multidimensional functions," *Journal of Optimization Theory and Applications*, vol. 145, no. 1, pp 120-147, Apr. 2010.
- [22] Test case data, [Online] Available: https://sites.google.com/site/leiwwpe s/data/TD Multi-port.zip.
- [23] L. Wu, "Accelerating NCUC via binary variable-based locally ideal formulation and dynamic global cuts," *IEEE Trans. Power Syst.*, vol. 31, no. 5, pp. 4097-4107, Sept. 2016.
- [24] J. Lofberg, "YALMIP: a toolbox for modeling and optimization in MATLAB," 2004 IEEE International Conference on Robotics and Automation, New Orleans, LA, USA, Sep. 2004.
- [25] IPOPT, [Online] Available: https://coin-or.github.io/Ipopt/.

BIOGRAPHIES

Yikui Liu (S'15) received the B.S. degree in electrical engineering and automation from Nanjing Institute of Technology, China, in 2012 and the M.S. degree in power system and automation from Sichuan University, China, in 2015.

He is currently pursuing the Ph.D. degree with Electrical and Computer Engineering Department, Stevens Institute of Technology, USA. His current research interests are power market and OPF in distribution system.

Lei Wu (SM'13) received the B.S. degree in electrical engineering and the M.S. degree in systems engineering from Xi'an Jiaotong University, Xi'an, China, in 2001 and 2004, respectively, and the Ph.D. degree in electrical engineering from Illinois Institute of Technology (IIT), Chicago, IL, USA, in 2008

From 2008 to 2010, he was a Senior Research Associate with the Robert W. Galvin Center for Electricity Innovation, IIT. He was a summer Visiting Faculty at NYISO in 2012. He was a Professor with the Electrical and Computer Engineering Department, Clarkson University, Potsdam, NY, USA, till 2018. He is currently a Professor with the Electrical and Computer Engineering Department, Stevens Institute of Technology, Hoboken, NJ, USA. His research interests include power systems operation and planning, energy economics, and community resilience microgrid.

Yonghong Chen (SM'12) received the B.S. degree from Southeast University, Nanjing, China, the M.S. degree from Nanjing Automation Research Institute, China, and the Ph.D. degree from Washington State University, Pullman, WA, USA, all in electrical engineering. She also received the M.B.A. degree from Indiana University, Kelly School of Business, Indianapolis, IN, USA. She is currently a Consulting Advisor at MISO. In this role, she focuses on R&D to address challenges on market design and market clearing system. Before joining MISO in 2002, she worked with GridSouth Transco LLC and Nanjing Automation Research Institute.

Jie Li (M'14) received the B.S. degree in information engineering from Xi'an Jiaotong University in 2003 and the M.S. degree in system engineering from Xi'an Jiaotong University, China in 2006, and the Ph.D. degree from the Illinois Institute of Technology (IIT), Chicago, in 2012.

From 2006 to 2008, she was a Research Engineer with IBM China Research Lab. From 2012 to 2013, she was a Power System Application Engineer with GE Energy Consulting. She was an Assistant Professor with the

11

Electrical and Computer Engineering Department, Clarkson University, Potsdam, NY, USA, during 2014 to 2019. She is currently an Associate Professor with the Electrical and Computer Engineering Department, Rowan University, Glassboro, NJ, USA. Her research interests include power systems restructuring and bidding strategy.

Yafei Yang (M'19) received the B.S. degree in electrical engineering and the Ph.D. degree in systems engineering from Xi'an Jiaotong University, Xi'an, China, in 2011 and 2017, respectively.

She is currently a postdoc of the Electrical and Computer Engineering Department at Stevens Institute of Technology. Her research interests include optimization scheduling of large-scale power systems and power system security analysis.